Sensor and Simulation Notes

Note 367

16 March 1994

Balantenna, Part II

Carl E. Baum
Phillips Laboratory

Donald P. McLemore
Kaman Sciences Corporation

Abstract

The balantenna combines two asymptotic bicones fed in series via a broadband (transient) balun (or transformer) achieving an impedance increase of 4:1 over the feeding coax. Going from a single-apex to a double-apex design allows two of the conducting cones that cover the center assembly to become flat faces. Then special transmission lines through the center assembly (and thereby through the choke) are used to divide the signal (in parallel) from the feeding coax to the two bicones.

I. Introduction

A balantenna, as introduced in [5] combines the propeerties of a balun and an antenna. As a balun in transmission it steps up the voltage as 1 : 2 and impedance as 1 : 4 (with the important practical case of 50 Ω : 200 Ω). The antenna consists of two conical antennas (each of 100 W characteristic impedance near the apex) connected in series via the center assembly which contains the choke (ferrite or similar). Let us refer to this as the single-apex design since both asymptotic bicones share a common apex. The center assembly has the covering conductors come back together smoothly outside the choke to preserve current continuity. The remaining two asymptotic cones (the outermost ones from each bicone) connect to the larger antenna which includes the 50 Ω coax bringing the signal to the balantenna, this coax being "hidden" as part of the wormhole feed [4].

As discussed in [7] one difficulty is associated with the ferrite with conical surfaces based on the same apex. The ferrite thickness is small near the apex which limits the power handling capability due to heating of the ferrite. If one could make this ferrite thickness greater this problem could be made smaller, and the choke impedance (inductive and resistive) could be made larger at the high frequencies of interest. As is discussed later this is accomplished by making the two asymptotic bicones have separated apices, allowing the choke material to have a shape more like a truncated circular cylinder (with a hole along the axis).

II. Feed Connections in Single Apex Design

Calling the two asymptotically conical conductors surrounding the choke material (e.g. ferrite) faces, then fig. 2.1 illustrates how the feeding coaxial conductors connect to the two faces, here labelled A and B. Note that the coaxial feed cable is itself contained within an asymptotic conical conductor labelled feed arm 1 in [5] and there is also a connection through to a similar conductor labelled antenna arm 2.

In [5] the connections were illustrated as single connections to A and B. Here there are two in each case which more uniformly distribute the current around the hole through the faces. Note also that the width of the flaring connections can be adjusted to better match the desired characteristic impedances. This technique is readily generalized to N connections to each face giving the view in fig. 2.1B with an N-fold rotation axis (C_N symmetry).

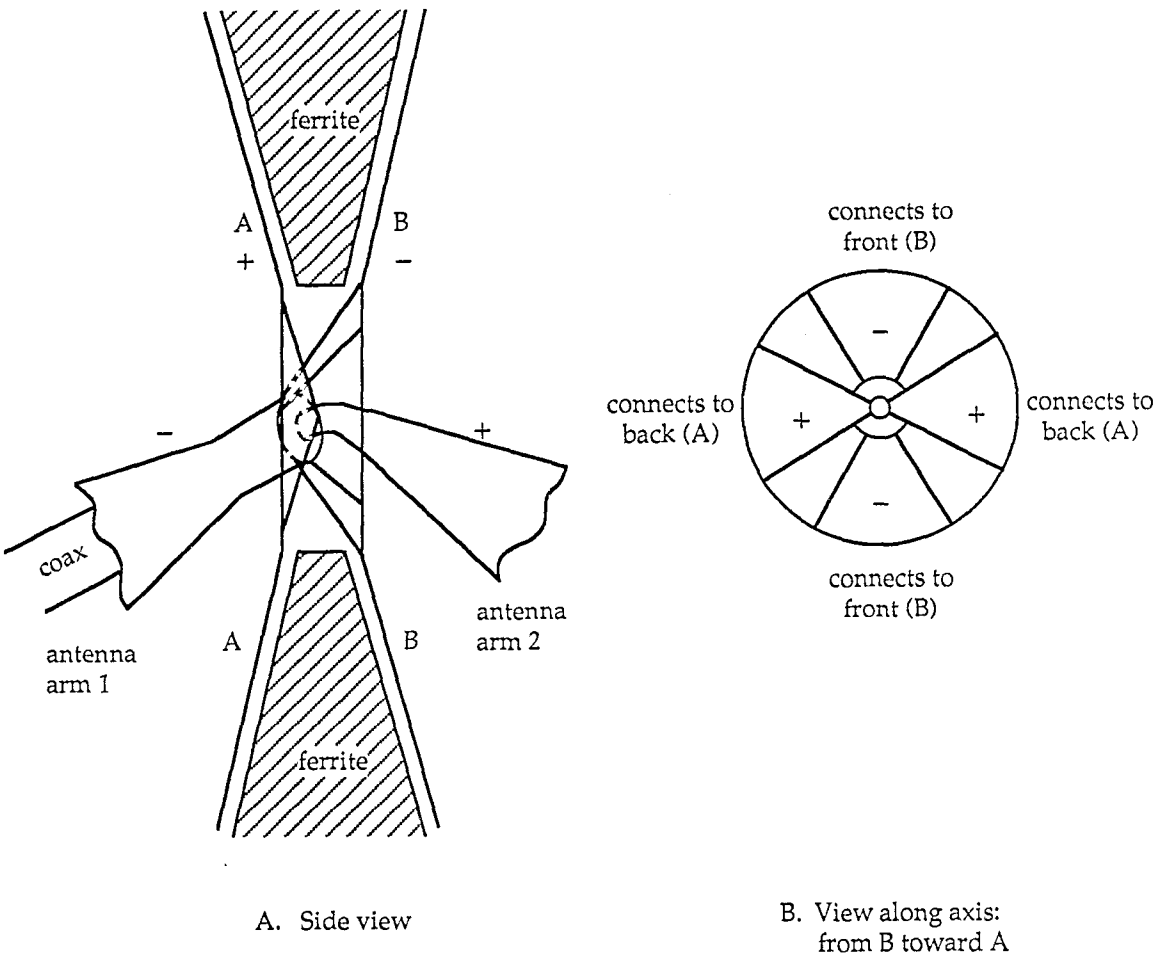

A. Side view

B. View along axis:
from B toward A

Figure 2.1 Internal Details for Single Apex: Two Electrical Connections Per Face

III. Feed Connections in Double Apex Design

Now consider a double apex design in which the two asymptotic bicones have apices separated along the axis (z axis as in [5]) at say $z = \pm d$. In fig. 3.1 this is illustrated with the convenient case that the two faces are taken as planar conducting sheets (perpendicular to the z axis). This allows the magnetic material to have flat surfaces just inside these faces. Note that this geometry is also appropriate for a hybrid of magnetic and dielectric sheets as discussed in [6].

With the two apices separated one has the problem of driving the two conical antennas (in asymptotic sense) with identical signals (adding in series). This can be accomplished by taking the coax from antenna arm 1 halfway between faces A and B in a circular hole through the center assembly. Then special transmission lines take the coax center conductor back to face A and the coax shield to face B. As illustrated in fig. 3.1 there are again two connections to each face, this being generalizable to N with C_N rotation symmetry. Going back toward A the additional transmission line involves two conductors outside the coax shield. Going toward B this takes the form of two conductors parallel to the extension of the coax center conductor. The details of these transmission lines are indicated by the views in B through F of fig. 3.1, to have twice the characteristic impedance of the coax (100 Ω for a 50 Ω coax), thereby matching to both the coax and asymptotic conical antennas.

Now these open transmission lines going to faces A and C can have the signal propagation affected by the presence of the ferrite. One may wish to confine the magnetic field away from this ferrite by making the cross sections of these lines (and of the coax) small compared to the hole diameter through the ferrite. Note that the two transmission lines and coax can be trimmed to allow for parasitic effects so that the signals arrive at faces A and B with exactly the same delay. If desired the right transmission line (connecting to B) can be made to look just like the left by using the shield of a piece of coax as the center conductor here.

An alternate configuration for these two transmission lines is to use a coaxial conductor as illustrated in fig. 3.2, effectively taking the limit as $N \to \infty$. This has the added advantage of confining the transmission-line mode interior to this coaxial shield. The ferrite then cannot affect the propagation of this mode. The characteristic impedance (double that of the feeding coax) and equal propagation times to the two faces are the important parameters of these transmission lines.

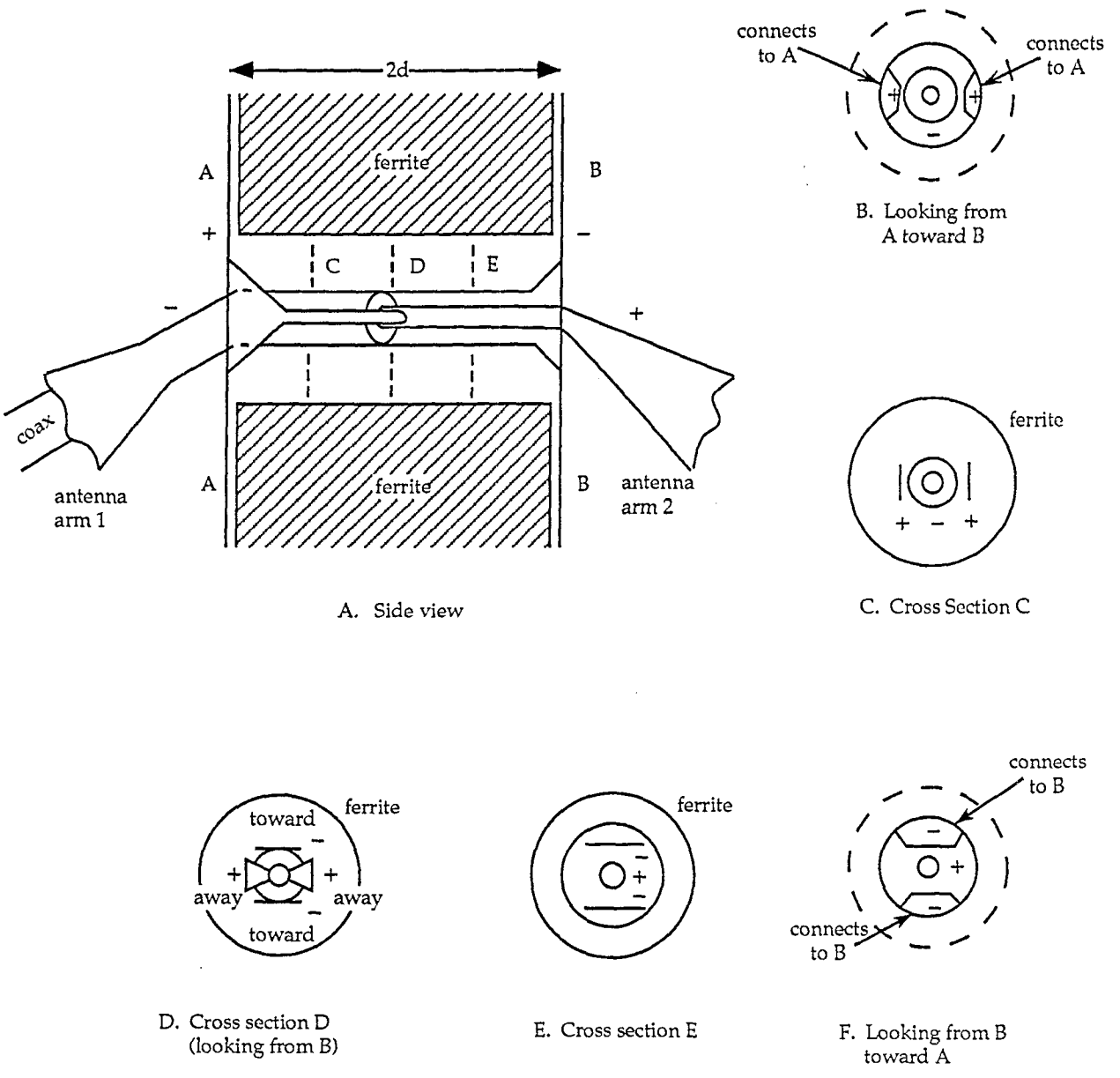

Figure 3.1 Internal Details for Double Apex: Two Electrical Connections Per Face

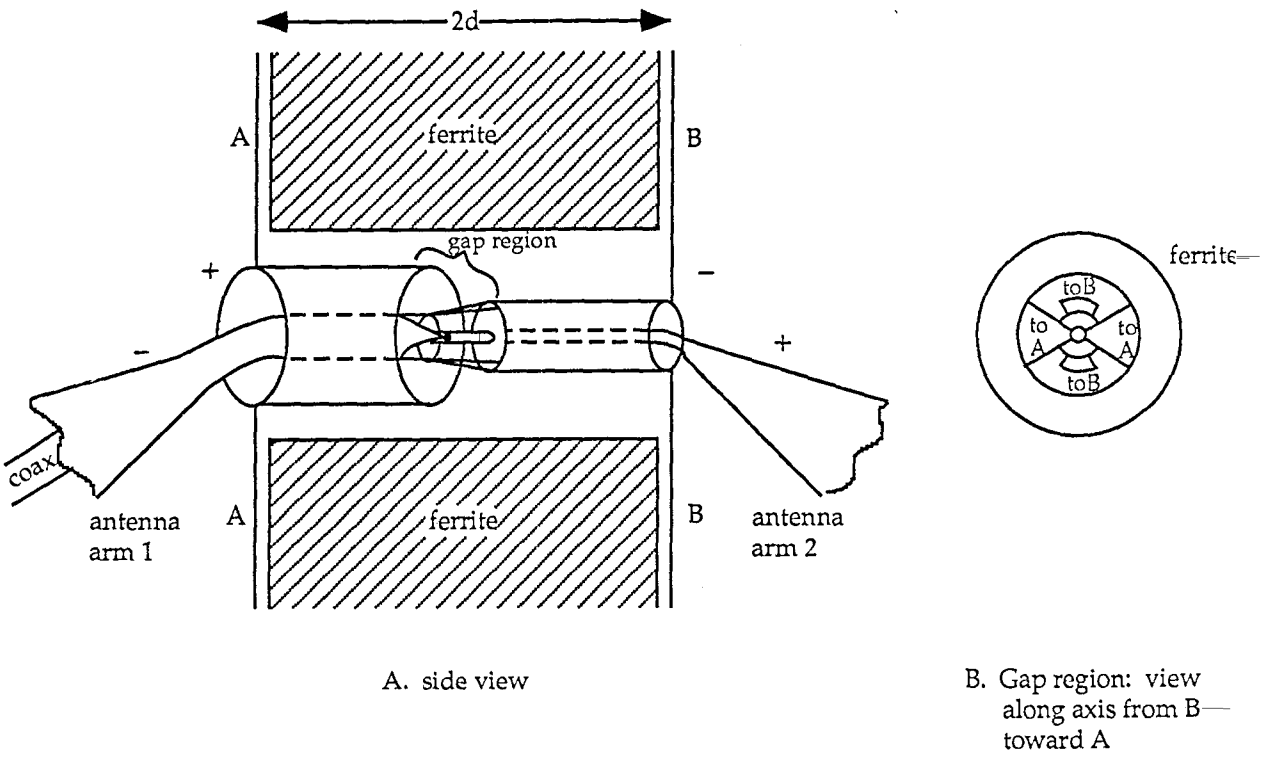

A. side view

B. Gap region: view along axis from B— toward A

Figure 3.2 Interior Details for Double Apex: Coaxial Transmission Lines to Faces

IV. Comparison of Antenna Characteristics

The single-apex design has some limitation on the high-frequency performance based on the thickness of the center assembly, $2d_1$ in fig. 4.1. Here let us take a simplified description. Instead of a smooth curved intersection with a plane of constant ϕ in a cylindrical (Ψ, ϕ, z) coordinate system, approximate the arcs by straight lines as indicated. The conical faces extend out to $\Psi = \Psi_1$ and from there taper back to where they meet at $\Psi = \Psi_2$ on the $z = 0$ plane. For convenience the antenna-arm portions are not included here, being described in previous illustrations.

Consider two rays going toward ∞ near the $z = 0$ plane $(\theta = \pi/2)$ labelled P_1 and P_1'. The thickness of the center assembly makes P_1 travel an extra distance (to go around the center assembly) of

$$\begin{aligned} \Delta_1 &= \left[\Psi_1^2 + d_1^2\right] - \Psi_1 \\ &\simeq \frac{d_1^2}{2\Psi_1} \text{ for } \frac{\pi}{2} - \theta_1 = \arctan\left(\frac{d_1}{\Psi_1}\right) \to 0 \end{aligned} \tag{4.1}$$

This can be made small by decreasing d_1 (for a given θ_1) but this limits the choke inductance. There is another extra distance for the P_1' path over the P_1 path of

$$\begin{aligned} \Delta_1' &= \left[\left[\Psi_2 - \Psi_1\right]^2 + d_1^2\right]^{\frac{1}{2}} - \left[\Psi_2 - \Psi_1\right] \\ &\simeq \frac{d_1^2}{2\left[\Psi_2 - \Psi_1\right]} \text{ for } \Psi_2 - \Psi_1 \to \infty \end{aligned} \tag{4.2}$$

This contribution can be made quite small by increasing Ψ_2. This last "dispersion distance" [1] is associated with diffraction at $(\Psi, z) = (\Psi_2, 0)$ and gives a significant effect for radian wavelengths of order Δ_1' or less. The former dispersion distance is associated with diffraction at $(\Psi, z) = (\Psi_1, d_1)$, which is limited by the angle θ_1.

The double-apex design has its rays to ∞ near the $z = 0$ plane illustrated on fig. 4.2. Corresponding to Δ_1 for the first portion of the ray, since face A is now parallel to the $z = 0$ plane, there is no extra distance Δ_2 for the wave to travel (for $0 < \Psi < \Psi_1$) giving

$$\Delta_2 = 0 \tag{4.3}$$

For $\Psi > \Psi_1$ the P_2' path has an extra distance compared to the P_2 path as

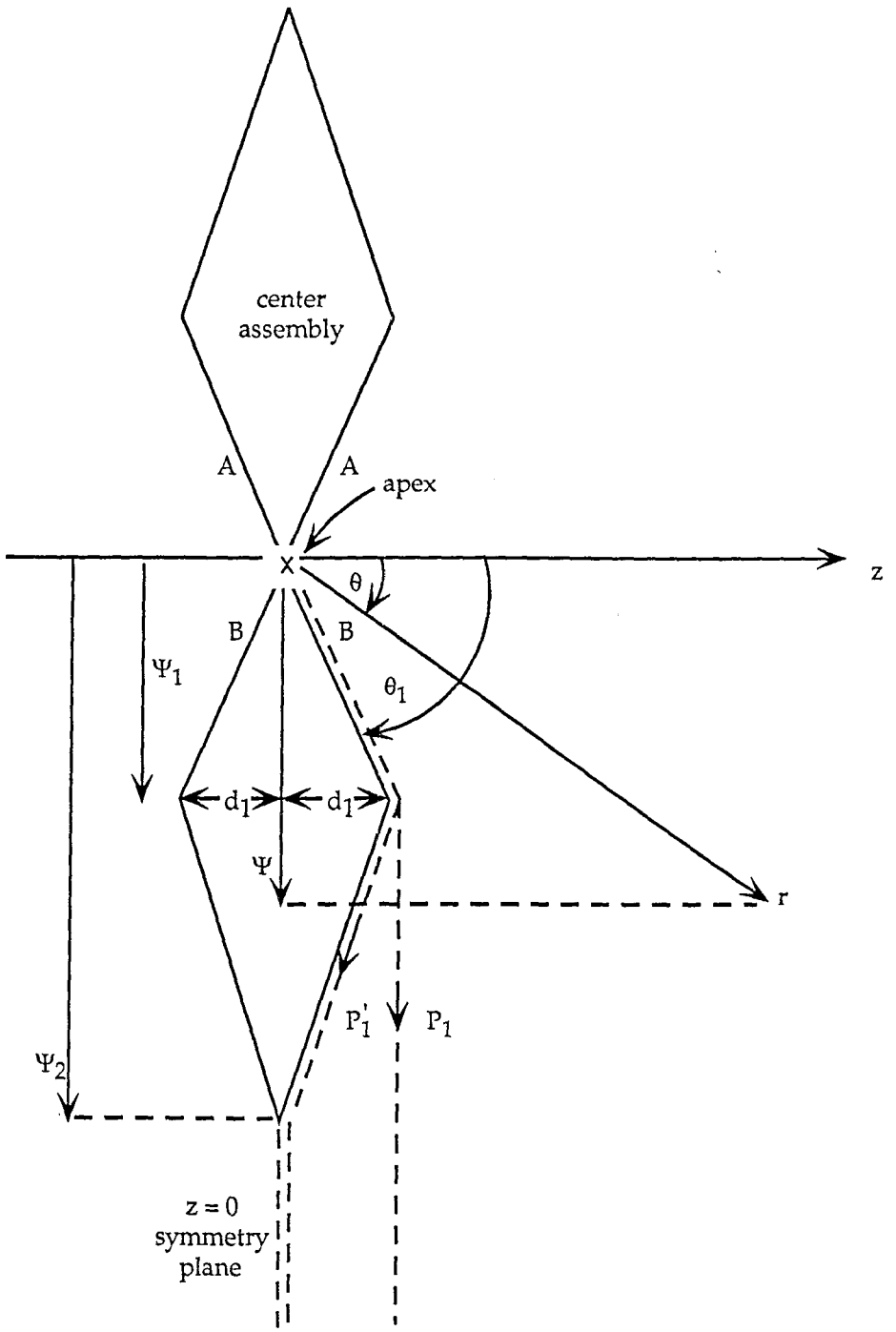

Figure 4.1 Path Difference on Symmetry Plane for Single-Apex Design

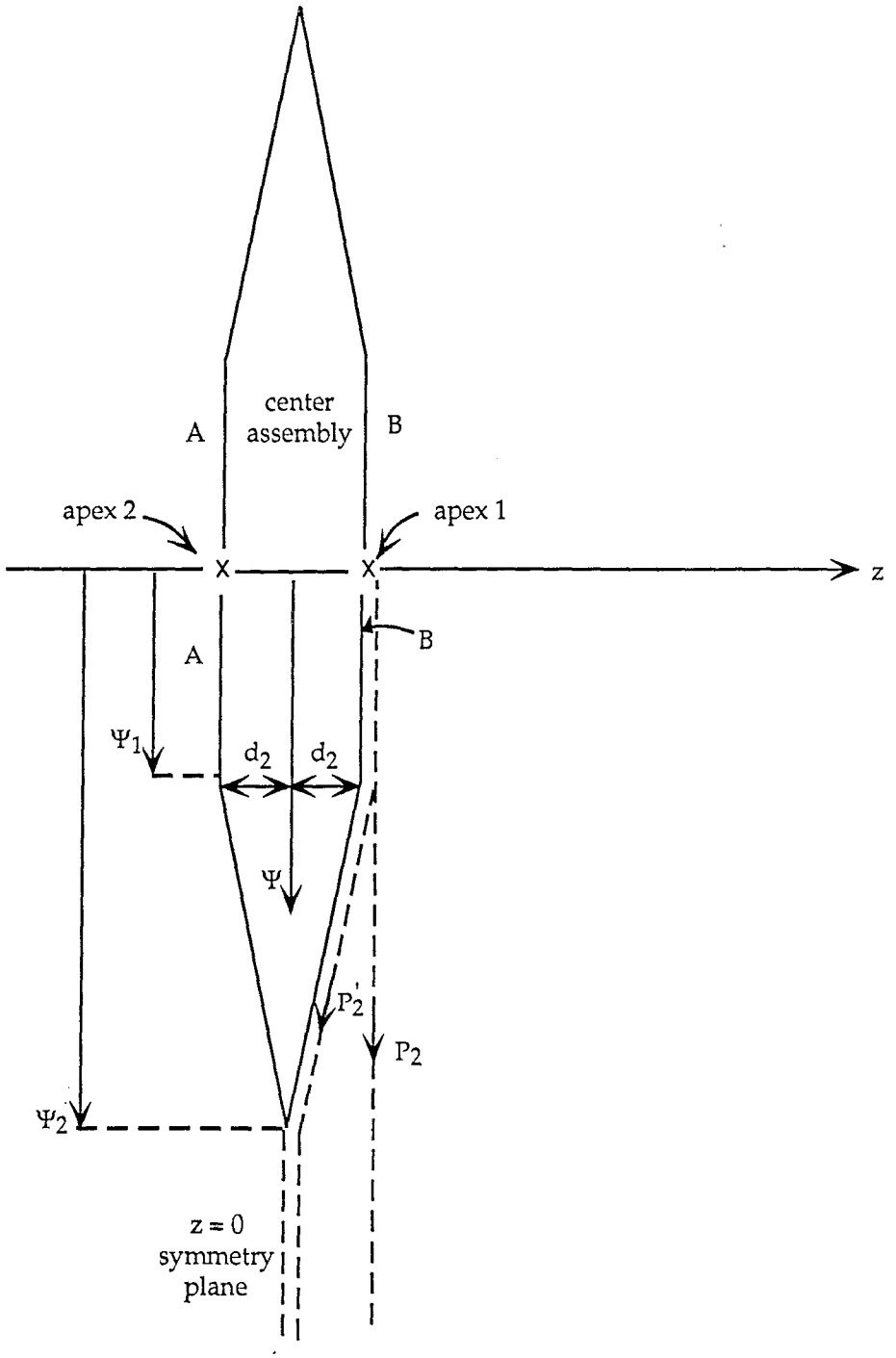

Figure 4.2 Path Difference on Symmetry Plane for Double-Apex Design

$$\Delta_2' = \left[\left[\Psi_2 - \Psi_1\right]^2 + d_2^2\right]^{\frac{1}{2}} - \left[\Psi_2 - \Psi_1\right]$$
$$\simeq \frac{d_2^2}{2\left[\Psi_2 - \Psi_1\right]} \text{ for } \Psi_2 - \Psi_1 \to \infty \tag{4.4}$$

which has the same form as Δ_1'. Note, however, that d_2 can be smaller than d_1 and still have a large choke impedance due to the greater thickness of the ferrite near the z axis (where this thickness counts even more due to the small Ψ for the hole radius through the ferrite). Noting also that Ψ_2 can be made large enough that Δ_2' can be made quite small, the high-frequency performance of the double apex design is better than that for the single apex design, except possibly for the transmission-line performance discussed in Section III.

Note that the radius Ψ_2 of the center assembly is quite important. For simplicity consider the case of two joined bicones as in fig. 4.3 in which the observer has a direct line of sight to both apices. If Ψ_2 is small compared to d_2, then for a large variation of θ (limited basically by an angle of the antenna arms) the observer has a line-of-sight view of both apices. When the differential distance for the two rays as in fig. 4.3 is

$$d_{2,1} = 2d_2 \cos(\theta) = \frac{\lambda}{2}$$
$$\lambda = \frac{c}{f} \equiv \text{wavelength}\ ,\ f \equiv \frac{\omega}{2\pi} \equiv \text{frequency} \tag{4.5}$$
$$c = \left[\mu_o \in_o\right]^{-\frac{1}{2}} \equiv \text{speed of light}$$

the signals arrive at the observer 180° out of phase, giving a null. Calling θ_1 (and $\pi - \theta_1$) some smallest angle of interest one can define a frequency for which a null first occurs within $\pi - \theta_1 \le \theta \le \theta_1$ as

$$f_1 \equiv \frac{c}{\lambda_1} \equiv \frac{c}{4d_2 \cos(\theta_1)} \text{ for } \theta \le \theta_1 < \frac{\pi}{2} \tag{4.6}$$

Now if θ_1 is constrained for our design this gives an expression for f_{max}, our bandwidth, as f_1. For

$$0 \le f < f_1 \tag{4.7}$$

there is no null. Now a bound on $|\cos(\theta_1)|$ is clearly 1, this providing a lower bound on f_1 as

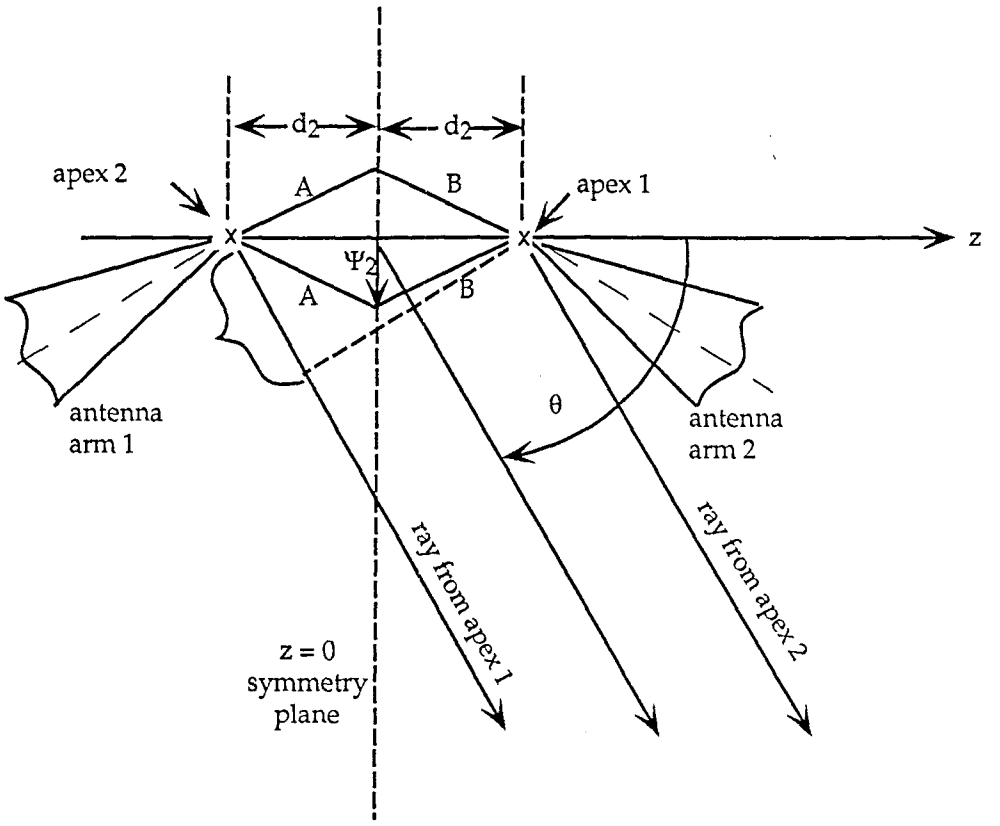

Figure 4.3 Double Apex with Thin Cones for Center Assembly

$$f_1 \geq \frac{c}{4d_1} \tag{4.8}$$

For a given d_1, then how does one get $f_{\max} > c/(4d_1)$, assuming this is desired? One technique is, of course, that of restricting θ_1 to regions away from 0, i.e., by keeping the range of θ near $\pi/2$, the symmetry plane. Suppose, however, some larger θ_1 is desired, say based on some test volume to be covered, with the volume at some finite specified distance from the source. Then θ_1 is a given, implying the result of (4.6). Is there still some way to raise f_{max} above this? To do this change the problem geometry.

Approximate the double-apex design by the double bicone in fig. 4.4. For simplicity let the two cones forming the center assembly be circular with half angle $\pi/2 - \theta_2$ where

$$\theta_2 = \arctan\left(\frac{d_2}{\Psi_2}\right) \tag{4.9}$$

can be a small angle. Comparing to fig. 4.2 note that for sufficiently large Ψ_2 / d_2 the faces of the center assembly are almost flat and can be approximated (or even constructed) by the circular cones in fig. 4.4. Using the techniques in [5, 8] one can readily calculate the characteristic impedance of the two bicones (equal by symmetry), including for non-zero θ_2.

Now suppose that $0 < \theta < \pi/2 - \theta_2$ (or equivalently $\pi > \theta > \pi/2 + \theta_2$). There is a direct ray (ray 1) from apex 1. There are two diffracted rays, 2a from apex 1 and 2b from apex 2, becoming ray 2 after joining at $(\Psi, z) = (\Psi_2, 0)$, the edge of the center assembly. For λ much less than Ψ_2 this diffraction coefficient is proportional to $f^{-\frac{1}{2}}$ which can be neglected for sufficiently high frequency. For small θ_2 this gets better and better, tending to zero as $\theta_2 \to 0$ due to the center assembly tending to be merely part of the symmetry plane. This says that there is no null in the θ direction under the above conditions. Note that frequencies of interest are only for $f > f_1$ for which $\lambda << \Psi_2$ provided θ_2 is small enough.

Then we only need to consider cases that have $|\pi/2 - \theta| < \theta_2$ for which we have direct rays from both apices. In this case we can use the previous results with θ_1 replaced by $\pi/2 - \theta_2$. So now define

$$f_2 \equiv \frac{c}{\lambda_2} \equiv \frac{c}{4d\cos\left(\frac{\pi}{2} - \theta_2\right)} \equiv \frac{c}{4d\sin(\theta_2)} \tag{4.10}$$

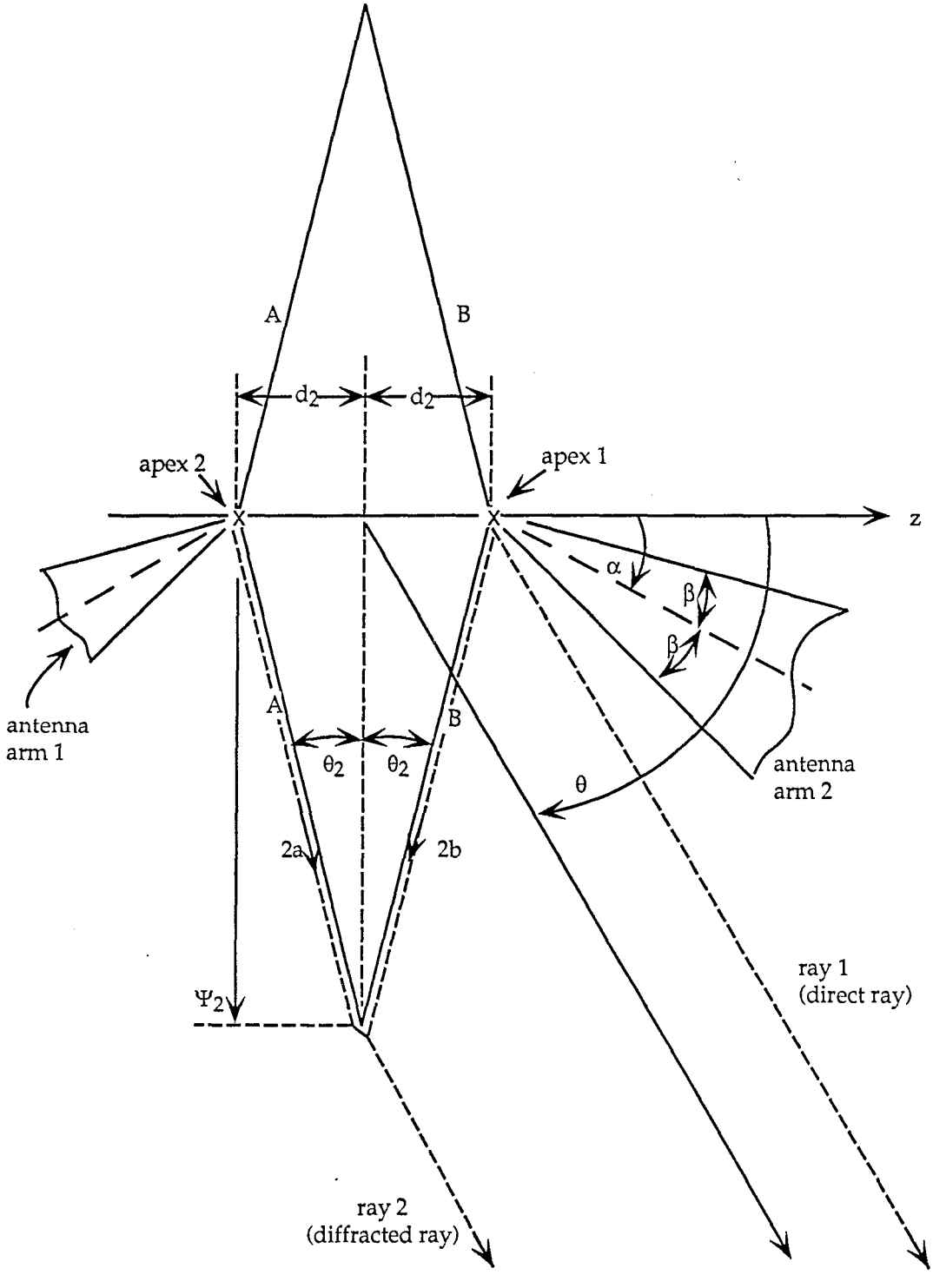

Figure 4.4 Double Apex with Large Center Assembly

On the direct-ray basis there is no null for

$$0 \leq f < f_2 \tag{4.11}$$

and note that

$$f_2 \to \infty \text{ as } \theta_2 \to 0 \tag{4.12}$$

so f_2 can be made *arbitrarily large.*

A related concept concerns the length of the input conical section of a guided-wave (e.g., parallel-plate) simulator [1]. As the length is made larger and larger the mode matching is better and better, in the limit giving an infinite bandwidth.

Consider the special case of $\theta = \pi/2$ for which there are two direct rays (parallel to the symmetry plane) to the observer, one from each apex. The diffracted rays, 2a and 2b in fig. 4.4 give a combined diffracted ray along the $z = 0$ plane to the observer. This diffracted ray takes a path with a length longer than the direct rays of amount (a dispersion distance)

$$\begin{aligned} \Delta_3 &= \left[d_2^2 + \Psi_2^2\right]^{\frac{1}{2}} - \Psi_2 = d_2\left[\csc(\theta_2) - \cot(\theta_2)\right] \\ &= d_2 \tan\left(\frac{\theta_2}{2}\right) \simeq d_2 \frac{\theta_2}{2} \end{aligned} \tag{4.13}$$

which can be compared to the similar expression in (4.2). For $\lambda >> \Delta_3$ the rays add in phase. As $\theta_2 \to 0$ the frequency where an interference can occur has $f \to \infty$. Since the symmetry plane can be taken as a perfectly conducting plane for our analysis, one can look at this problem as a small interior bend in a ground plane [2, 3]. In this latter case account should be taken of the spherical nature of the incident wave.

V. Impedance of Each Bicone

The results of [5] are directly applicable to the present case with flat faces for the center assembly (fig. 4.2). In the notation of [5] we have

$$\begin{aligned} \chi &\equiv \frac{\pi}{2} - \theta_1 \quad \text{(in fig. 4.1)} \\ \alpha &\equiv \text{angle between } z \text{ axis and axis of antenna arm 2 (a circular cone) (fig. 4.4)} \\ \beta &\equiv \text{half angle of each antenna arm (angle between axis and surface of circular cone) (fig. 4.4)} \end{aligned} \tag{5.1}$$

The characteristic impedance of each bicone (noting two in series) is

$$\begin{aligned} Z_c &= Z_o f_g \ , \ Z_o \equiv \sqrt{\frac{\mu_o}{\epsilon_o}} \\ f_g &= \frac{1}{2\pi} \operatorname{arccosh}\left(\frac{\cos(\alpha) - \sin(\chi)\cos(\beta)}{\cos(\chi)\ \sin(\beta)}\right) \end{aligned} \tag{5.2}$$

where ζ has been replaced in terms of χ in [5].

Now considering our case of interest with flat faces for the center assembly we have

$$\begin{aligned} \chi &= 0 \quad \text{(flat face)} \\ f_g &= \frac{1}{2\pi} \operatorname{arccosh}\left(\frac{\cos(\alpha)}{\sin(\beta)}\right) \end{aligned} \tag{5.3}$$

This is readily inverted as

$$\frac{\cos(\alpha)}{\sin(\beta)} = \cosh\left(2\pi f_g\right) \tag{5.4}$$

from which for a given f_g (say for 100 Ω) one can readily find acceptable choices (pairs) of α and β. This result is plotted in fig. 5.1 for various choices of this bicone impedance.

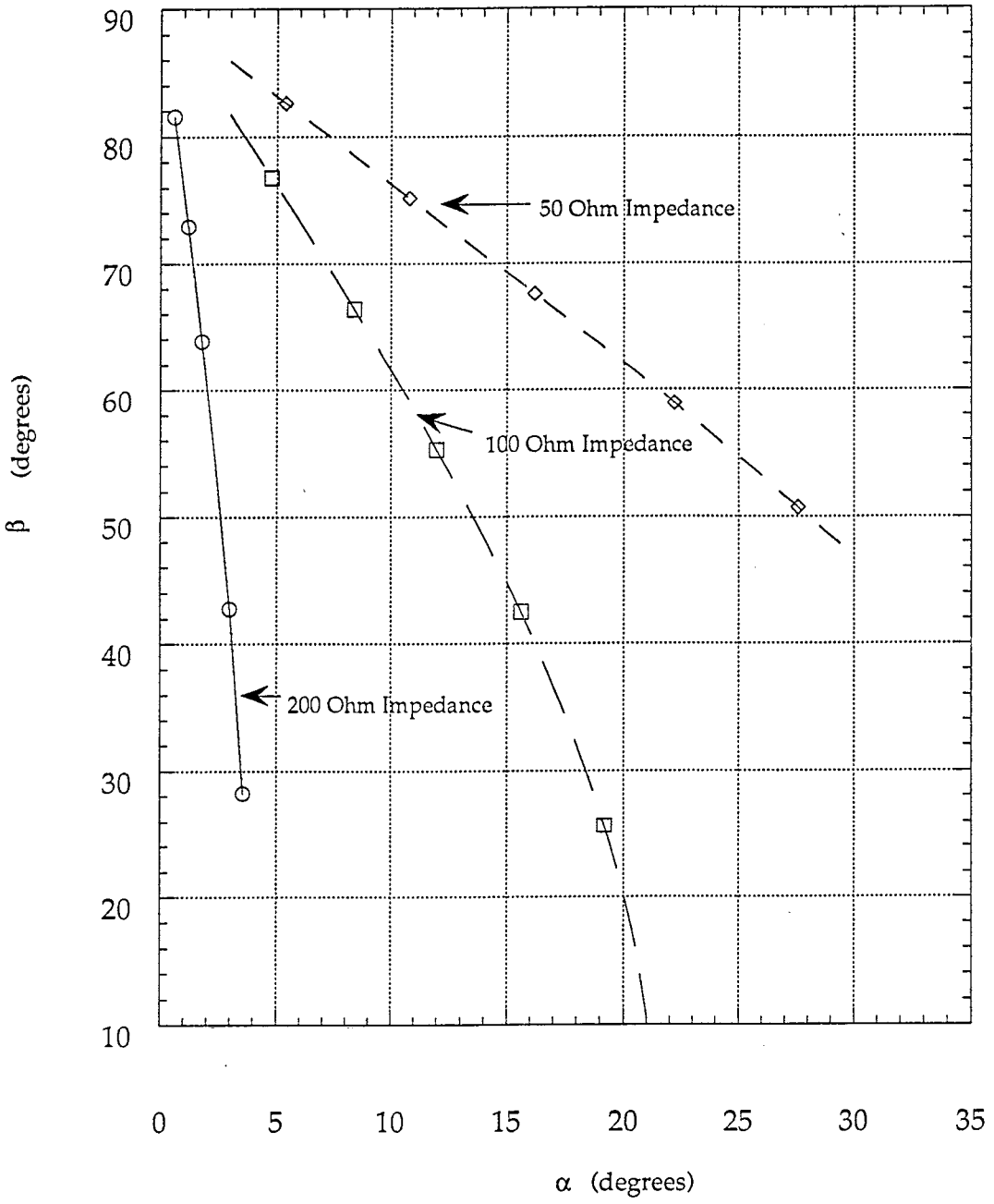

Figure 5.1 Combinations of Angles for a Given Bicone Impedance

VI. Concluding Remarks

This paper gives some design options for the balantenna. From an antenna standpoint the double apex is better than a single apex. One may be concerned about the fact that there are two "phase centers" and how one interprets this in terms of a spherical wave. However, if we take the point of view that we are trying to approximate a plane wave, then this characteristic is not significant. This advantage of the double-apex design should be contrasted with the added complexity associated with the transmission lines passing through the center assembly. So some trade off is called for to achieve optimum performance.

References

1. C. E. Baum, The Conical Transmission Line as a Wave Launcher and Terminator for a Cylindrical Transmission Line, Sensor and Simulation Note 31, January 1967.

2. C. E. Baum, The Diffraction of an Electromagnetic Plane Wave at a Bend in a Perfectly Conducting Planar Sheet, Sensor and Simulation Note 47, August 1967.

3. D. F. Higgins, The Diffraction of an Electromagnetic Plane Wave by Interior and Exterior bends in a Perfectly Conducting Sheet, Sensor and Simulation Note 128, January 1971.

4. C. E. Baum, W. D. Prather, and D. P. McLemore, Topology for Transmitting Low-Level Signals from Ground Level to Antenna Excitation Position in Hybrid EMP Simulators, Sensor and Simulation Note 333, September 1991, and Proc. 10th Int'l. Zurich Symposium and Technical Exhibition on Electromagnetic Compatibility, 1993, pp. 359-362.

5. D. P. McLemore, G. D. Sower, C. E. Baum, and W. D. Prather, The Balantenna: An Integrated Impedance Matching Network and Hybrid EMP Simulator, Sensor and Simulation Note 355, January 1993.

6. C. E. Baum, An Anisotropic Medium for High Wave Impedance, Measurement Note 39, May 1991.

7. G. D. Sower, Baluns for Driving High Power Levels from 50 Ohm Amplifiers/Cables into High Impedance Antennas/Loads, Measurement Note 45, October 1993.

8. R. W. Latham, M.I. Sancer, and A. D. Varvatsis, Matching a Particular Pulser to a Parallel-Plate Simulator, Circuit and Electromagnetic System Design Note 18, November 1974.